31st EPS Conference on Plasma Phys. London, 28 June - 2 July 2004 ECA Vol.**28G**, P-2.062 (2004)

Dynamics of convection around axisymmetric magnetic flux tubes

G.J.J. Botha[1], A.M. Rucklidge[1], N.E. Hurlburt[2]

[1] *Department of Applied Mathematics, University of Leeds, Leeds LS2 9JT, UK*

[2] *Lockheed Martin Solar and Astrophysics Laboratory, Palo Alto CA 94304, USA*

Pores and sunspots are some of the magnetic features observed on the surface of the solar photosphere. Magnetic flux is pushed to boundaries between convection cells (granules), where they form flux elements that have a lifetime of a few minutes, field strengths of 1500G and magnetic fluxes in the order of 0.0001TWb. The flux elements collect at the corners of supergranules (where the surface flows converge) and the magnetic field strength grows (possibly) to form pores. Pore sizes range from 2000 – 4000km, with field strengths of approximately 2000G and magnetic fluxes of up to 7TWb. This field strength seems not to depend on pore size. Pores may grow into sunspots. Most sunspots tear apart within a few hours, but some have lifetimes of several weeks and grow to diameter sizes of up to 50,000km. Their field strengths can be up to 3000G in the umbra and 1500G in the penumbra, with magnetic flux varying between 2 – 200TWb. The sunspot penumbra has a surface flow radially outward from the sunspot (Evershed flow), which is slightly elevated above the rest of the photosphere. The supergranular cell around a sunspot and its penumbra is called the moat cell, and features outward convection. In this presentation a numerical model is used to study idealised pores and sunspots. Vertical flux tubes are placed in a compressible convecting photosphere in an axisymmetric cylindrical box with radius up to 4 times its depth [1]. The numerical box is initialised with a temperature and density stratification

$$T = T_0(1 + \theta z) \qquad \text{and} \qquad \rho = \rho_0(1 + \theta z)^m, \tag{1}$$

with the 0 subscript defining the quantity at the top of the box ($z = 0$), θ the initial temperature gradient, and m the polytropic index ($T_0 = 1$, $\rho_0 = 1$). Fully compressible, nonlinear axisymmetric magnetoconvection is solved, using equations [2]

$$\frac{\partial \rho}{\partial t} = -\nabla \cdot (\mathbf{u}\rho) \,, \tag{2}$$

$$\frac{\partial \mathbf{u}}{\partial t} = -\mathbf{u}\cdot\nabla\mathbf{u} - \frac{1}{\rho}\nabla P + \theta(m+1)\hat{\mathbf{z}} - \frac{\sigma\zeta_0 K^2 Q}{\rho}\mathbf{j}\times\mathbf{B} + \frac{\sigma K}{\rho}\nabla\cdot\tau \ , \quad (3)$$

$$\frac{\partial T}{\partial t} = -\mathbf{u}\cdot\nabla T - (\gamma-1)T\nabla\cdot\mathbf{u} + \frac{\gamma K}{\rho}\nabla^2 T + \frac{\sigma K(\gamma-1)}{\rho}\left(\frac{1}{2}\tau:\tau + \zeta_0^2 Q K^2 j^2\right), \quad (4)$$

$$\frac{\partial A}{\partial t} = (\mathbf{u}\times\mathbf{B})_\phi - \zeta_0 K(\nabla\times\mathbf{B})_\phi \ , \quad (5)$$

with auxiliary equations

$$P = \rho T \ , \qquad \mathbf{B} = \nabla\times(\hat{\phi}A) \ , \qquad \nabla\cdot\mathbf{B} = 0 \ , \qquad \mathbf{j} = \hat{\phi}(\nabla\times\mathbf{B})_\phi \ , \quad (6)$$

and where τ is the rate of strain tensor, γ the ratio of specific heats, σ the Prandtl number, K the dimensionless thermal conductivity, ζ_0 the magnetic diffusivity ratio at $z = 0$, and Q the Chandrasekhar number. All other symbols have there usual meaning.

The numerical domain is a 2D representation (r, z) of an axisymmetric cylinder with radius Γ. On the axis ($r = 0$) the boundary conditions are

$$\frac{\partial \rho}{\partial r} = U_r = \frac{\partial U_z}{\partial r} = A = B_r = \frac{\partial B_z}{\partial r} = j = \frac{\partial T}{\partial r} = 0. \quad (7)$$

At $r = \Gamma$ the boundary is a slippery, perfectly conducting, thermally insulating wall. At the bottom boundary ($z = 1$) the temperature is fixed and the magnetic field is vertical. A potential field is placed at the top boundary ($z = 0$) together with a temperature governed by Stefan's law. The equations are evolved using fourth-order Bulirsch-Stoer time integration and sixth-order compact finite differencing [3]. We have explored the following parameter values:

$$10^5 \le R \le 10^7 \ ; \qquad 0.1 \le \sigma \le 0.3 \ ; \qquad 10 \le Q \le 10^4 \ ; \qquad 0.02 \le \zeta_0 \le 0.2 \ ;$$
$$(\gamma, m) = (\frac{5}{3}, 1.45) \ ; \ (\frac{5}{3}, 1.495) \ ; \ (\frac{5}{4}, 3.9975) \ ;$$

and $\theta = 10$. For the values used in Figure 1, the temperature increases by a factor of 11 in the vertical direction, and the density by a factor of 55.

We found anti-clockwise (inward flow at the top) and clockwise (outward flow) convection cells – which may respectively give an indication of processes associated with pores and the perumbral flow around sunspots. Figure 1 is an example of clockwise rotation. With such a convection cell, there is always a smaller anti-clockwise rotating cell forming at the left hand side of the large convection cell, which is time dependent. The fluctuation of the smaller cell shows periodic behaviour, seen clearly in the plasma

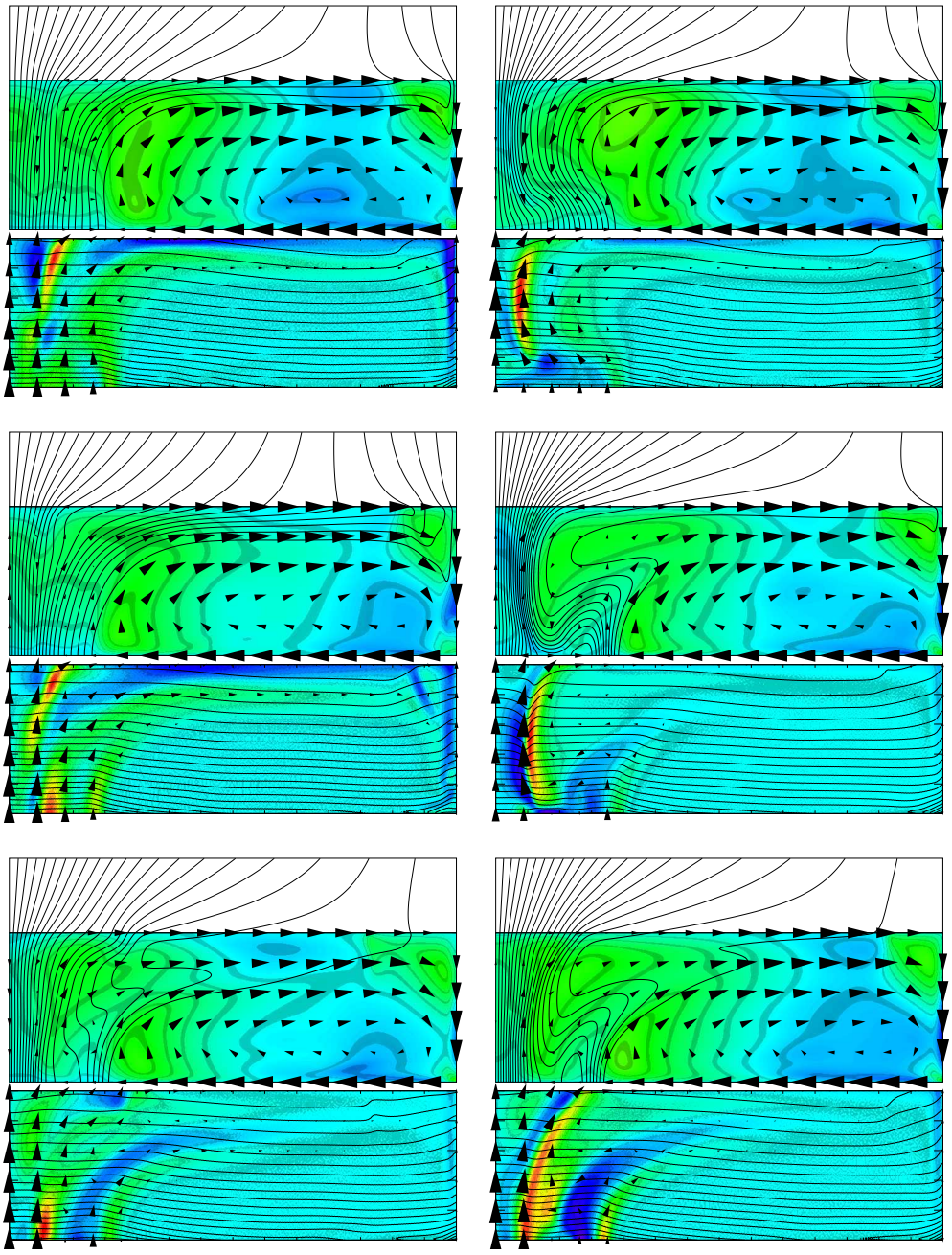

Figure 1: The six 2D plots show a time sequence in the clockwise direction, which is the same direction as movement in the main convection cell. Each plot consists of three boxes in the (r, z) plane. The top (black and white) box is the potential field. The middle box shows the magnetic field lines as contours, the temperature in colour and the velocity as arrows. The bottom box shows the magnetic field strength as arrows, the density as contour lines and the current in the ϕ direction in colour. These results were obtained with parameter values $R = 10^6$, $Q = 100$, $\sigma = 0.1$, $\zeta_0 = 0.2$, $m = 1.45$, and $K = 0.529$.

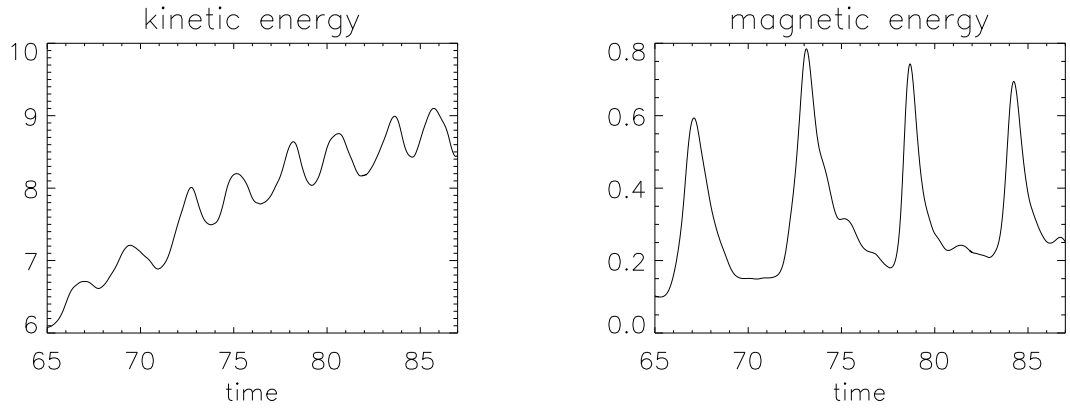

Figure 2: Kinetic and magnetic energy during evolution of clockwise convection cell.

kinetic and magnetic energy (Figure 2). As the small anti-clockwise cell forms, it pulls magnetic field lines and a plume of colder plasma to the bottom of the box. Once the field lines have moved underneath the cell, they are convected in the r direction towards $r = \Gamma$. With this action the anti-clockwise cell is destroyed, and the cycle repeats itself. The increase in kinetic energy in Figure 2 is due to the slow growth of the large clockwise convection cell. The peaks in magnetic energy correspond to the formation of the small anti-clockwise cell. With its destruction magnetic energy decreases.

The structure of the flows was investigated in terms of the possible influence of the numerical boundaries of the domain. At the top boundary, the potential magnetic field was replaced by a uniform (in z direction) magnetic field, while Stefan's law was replaced by a fixed temperature T_0. Neither of these changes influenced the convection in any significant way. The radius (Γ) of the numerical box was a deciding factor. For $\Gamma > 3$ more than one large convection cell formed, with the largest next to the strong magnetic field at $r = 0$ and rotating in an anti-clockwise direction. The physical parameters influencing the convection the most are Q and R. A large R causes strong convection currents to sweep the magnetic field lines with the flow, while a strong Q tends to inhibit convection. This inhibition takes the form of many smaller convection cells forming between the field lines. Numerical constraints have prevented us from increasing θ and m to large values.

[1] N.E. Hurlburt & A.M. Rucklidge, 2000, MNRAS **314**, 793-806.

[2] N.E. Hurlburt & J. Toomre, 1988, ApJ **327**, 920-32.

[3] S.K. Lele, 1992, Journal of Computational Physics, **103**, 16-42.